

Macroeconomic Uncertainty and Forecasting Macro- economic Aggregates

Magnus Reif

Impressum:

ifo Working Papers

Publisher and distributor: ifo Institute – Leibniz Institute for Economic Research at the University of Munich

Poschingerstr. 5, 81679 Munich, Germany

Telephone +49(0)89 9224 0, Telefax +49(0)89 985369, email ifo@ifo.de

www.cesifo-group.de

An electronic version of the paper may be downloaded from the ifo website:

www.cesifo-group.de

Macroeconomic Uncertainty and Forecasting Macroeconomic Aggregates

Abstract

Can information on macroeconomic uncertainty improve the forecast accuracy for key macroeconomic time series for the US? Since previous studies have demonstrated that the link between the real economy and uncertainty is subject to nonlinearities, I assess the predictive power of macroeconomic uncertainty in both linear and nonlinear Bayesian VARs. For the latter I use a threshold VAR that allows for regime-dependent dynamics conditional on the level of the uncertainty measure. I find that the predictive power of macroeconomic uncertainty in the linear VAR is negligible. In contrast, using information on macroeconomic uncertainty in a threshold VAR can significantly improve the accuracy of short-term point and density forecasts, especially in the presence of high uncertainty.

JEL Code: C11, C53, C55, E32

Keywords: Forecasting, BVAR, nonlinearity, threshold VAR, uncertainty

Magnus Reif
ifo Institute – Leibniz Institute for
Economic Research
at the University of Munich
Poschingerstr. 5
81679 Munich, Germany
reif@ifo.de

1 Introduction

Since the seminal contribution of Bloom (2009), the contractive effects of uncertainty shocks on the real economy are uncontroversial.¹ Moreover, recent studies show that uncertainty shocks have nonlinear effects. On the one hand, uncertainty shocks induce stronger effects during recessionary episodes or in times of financial distress (see, for instance, Caggiano, Castelnuovo and Groshenny, 2014; Ferrara and Guérin, 2018; Alessandri and Mumtaz, 2018). On the other hand, the magnitude of the variables' response to the uncertainty shock depends on the shock's sign (Jones and Enders, 2016; Foerster, 2014). While a great deal of the literature focus on structural analysis of fluctuations in uncertainty, evidence regarding the impact of uncertainty on forecast performance is, however, rather sparse.

This paper explores the link between economic uncertainty and forecast performance, making two contributions to the literature. First, I assess the predictive power of uncertainty in a linear model. I derive the baseline results using the large Bayesian VAR (BVAR) approach introduced by Bańbura, Giannone and Reichlin (2010).² The impact of economic uncertainty on forecast performance is assessed by adding a recursively estimated version of the macroeconomic uncertainty index of Jurado, Ludvigson and Ng (2015) to a medium-sized dataset of macroeconomic indicators for the US. Second, I investigate whether allowing for nonlinearity improves forecast accuracy relative to standard, linear models. To this end, I employ a threshold BVAR (T-VAR) that accounts for nonlinear relations between macroeconomic uncertainty and the real economy. This model allows to directly link the nonlinearity to the threshold variable, which in my application is the uncertainty index mentioned above.³ Moreover, the T-VAR facilitates the possibility of two distinct regimes, which can be interpreted as high and low uncertainty regimes. Since these regimes can differ in all of the model's parameters, the model allows for regime-dependent shock propagation processes and heteroscedasticity. As shown by several studies (for example, Barnett, Mumtaz and Theodoridis, 2014; Clark and Ravazzolo, 2015; Alessandri and Mumtaz, 2017), although not in the context of uncertainty, both features can significantly increase forecast accuracy. To estimate the threshold VAR, I combine the Gibbs sampler provided by Chen and Lee (1995) with the large Bayesian VAR framework mentioned above and the hyperparameter estimation approach of Giannone, Lenza and Primiceri (2015). The appealing property of this approach is that each of the model's parameters, including the tightness of the prior on the model coefficients, the lag of the threshold variable, as well as the threshold level (and therefore the regimes) are estimated endogenously and are purely data driven.

First, I perform an in-sample analysis based on quarterly US data from 1960 to 2017 to demonstrate that the T-VAR yields reasonable full-sample estimates. I illustrate that the estimated high uncertainty regimes are similar, but do not fully coincide with the recession dates provided by the NBER business cycle dating committee. Using the threshold BVAR, I isolate

¹For the transmission of uncertainty shocks to the real economy, capital adjustment frictions (Bernanke, 1983; Caballero and Pindyck, 1996; Bachmann and Bayer, 2013) and financial frictions (Gilchrist, Sim and Zakrajšek, 2014; Christiano, Motto and Rostagno, 2014; Arellano, Bai and Kehoe, 2012) have been found to be important.

²The large BVAR has been proven capable of processing a large number of economic indicators while generating precise forecasts (see Carriero, Kapetanios and Marcellino, 2009; Koop, 2013, among others).

³As shown in Section 4 of this paper, recessions and phases of high uncertainty do not inevitably coincide, which is why I do not condition the model on recessions.

state-dependent uncertainty shocks. To account for the model’s nonlinearity, I compute generalized impulse responses à la Koop, Pesaran and Potter (1996) with the modification of Kilian and Vigfusson (2011) that allows for nonlinear shock propagation. I show that the model is able to generate the effects of uncertainty shocks commonly found in the literature. I find that uncertainty shocks have both negative effects on the real economy and nonlinear effects, depending on the level of the uncertainty proxy. During episodes of high uncertainty, the effects of an uncertainty shock on labor market variables are much stronger. The peak response of the unemployment rate, for instance, is roughly twice the size in times of high uncertainty compared to normal times.

I conduct a rigorous out-of-sample forecast exercise using a recursive estimation scheme that mimics the information set of the actual forecaster at each point in time. I evaluate the forecasts with respect to both point forecasts and predictive densities. The point forecasts are evaluated in terms of mean forecast errors and root mean squared forecast errors. The predictive densities are evaluated using log predictive scores and continuous ranked probability scores.

My main results are that information on economic uncertainty can improve forecast accuracy and that density forecasts benefit more from this information than point forecasts. Concerning the point forecasts, I find that adding the uncertainty proxy to the otherwise standard linear BVAR yields only marginal improvements. Although, in most cases, the T-VAR is outperformed by the linear specifications, interest and unemployment rate forecasts can be significantly improved. With regard to the predictive densities, the linear models are dominated by the T-VAR. Indeed, in most cases, each model overestimate the true uncertainty of the data, indicated by too wide predictive densities. Controlling for uncertainty regimes, though, reduces this bias and provides a better description of the data. This suggests that accounting for state-dependent disturbances is more important for forecasting purposes than state-dependent shock propagation. Finally, I document substantial variation of the model’s predictive abilities over time and show that the gains in forecast accuracy are particularly high when uncertainty is high. Thus, the T-VAR can serve as a complement to existing approaches to get a better picture of the actual uncertainty surrounding the point estimate in times of high uncertainty.

This paper adds to the literature investigating the predictive power of uncertainty indicators. Pierdzioch and Gupta (2017) and Balcilar *et al.* (2016) focus on forecasting recessions and show that information on uncertainty improves forecast accuracy. Segnon *et al.* (2018) and Bekiros, Gupta and Paccagnini (2015) employ bivariate models including information on uncertainty and suggest that uncertainty can be helpful in predicting GNP growth and oil prices already in small-scale models. None of these contributions considers a large set of indicators that an applied forecaster would use, or directly allows for nonlinearity with respect to the uncertainty measure.

The paper is structured as follows. Section 2 describes the Bayesian VAR as well as the Bayesian threshold VAR and outlines the estimation methodology. Section 3 describes the dataset and the forecast methodology. Section 4 presents the in-sample results. Section 5 discusses the results from the forecast experiment. Section 6 concludes.

2 The Models

In this section, I first describe a standard Bayesian VAR model, following which the Bayesian threshold VAR is outlined.

2.1 The Bayesian VAR

The VAR(p) is specified as follows:

$$y_t = c + \sum_{j=1}^p A_j y_{t-j} + \varepsilon_t \quad \text{with } \varepsilon_t \sim N(0, \Sigma), \quad (1)$$

where y_t and c are $n \times 1$ vectors of endogenous variables and intercept terms, respectively. ε_t denotes the vector of normally distributed residuals. A_j are $n \times n$ matrices of coefficients with $j = 1, \dots, p$. I employ Bayesian estimation techniques to estimate the model. Specifically, I use the Minnesota prior developed by Litterman (1986), which assumes that every economic time series can be sufficiently described by a random walk with drift. Thus, the prior shrinks all coefficients on the main diagonal of A_1 towards one while the remaining coefficients are shrunk towards zero. Moreover, the classical Minnesota prior assumes a diagonal covariance matrix of the residuals. In the following, I use the generalized version of the classical Minnesota prior provided by Kadiyala and Karlsson (1997), which allows for a non-diagonal residual covariance matrix while retaining the idea of the Minnesota prior described above. As demonstrated by Bańbura *et al.* (2010), using a normal-inverse Wishart prior generates accurate forecasts despite the additional parameters to be estimated. In addition, I follow Doan, Litterman and Sims (1984) as well as Sims (1993) by implementing the ‘‘sum-of-coefficients’’ and ‘‘co-persistence’’ prior. The former accounts for unit roots in the data; the latter introduces beliefs on cointegration relations among the series. Each prior is implemented using dummy observations. I estimate the tightness of the priors by applying the hierarchical Bayesian procedure of Giannone *et al.* (2015). For details regarding the prior implementation and the estimation procedure, see Appendices A and B.

2.2 The Bayesian Threshold VAR

The threshold VAR is defined as follows:

$$y_t = \left(c_1 + \sum_{i=1}^p A_{1,i} y_{t-i} + \Omega_1^{0.5} \varepsilon_t \right) S_t + \left(c_2 + \sum_{i=1}^p A_{2,i} y_{t-i} + \Omega_2^{0.5} \varepsilon_t \right) (1 - S_t) \quad (2)$$

$$\text{with: } S_t = \begin{cases} 1, & \text{if } r_{t-d} \leq \bar{r} \\ 0, & \text{if } r_{t-d} > \bar{r} \end{cases} \quad (3)$$

where y_t is the vector of endogenous variables. Contrary to the linear VAR in (1), the intercept terms c_j and the matrices of coefficients A_j with $j \in \{1, 2\}$ are state dependent. The regime prevailing in period t depends on whether the level of the threshold variable, r , in period $t-d$ is below/above a latent threshold level, \bar{r} . This mechanism allows for different model dynamics

depending on the respective regime. As in the previous section, I use natural conjugate priors for the VAR coefficients and implement the priors using dummy observations. Moreover, the elements of Λ are separately estimated for both regimes to obtain a sensible degree of shrinkage. I follow Chen and Lee (1995) for the threshold level and the delay coefficient:

$$p(d) = \frac{1}{d_{\max}} \quad \text{and} \quad r^* \sim U(a, b), \quad (4)$$

where $d_{\max} = 8$ denotes the maximal delay. Since both the threshold value \bar{r} and the delay coefficient d depend on the model parameters and Λ_j depends on \bar{r} and d , the algorithm from the previous section is no longer appropriate. In fact, I combine the Metropolis Hastings step for estimating the amount of shrinkage (see Appendix B) with the Gibbs sampler introduced by Chen and Lee (1995) to simulate the posterior distribution of the model's parameters. In detail, the Gibbs sampler works as follows:

1. At iteration $k = 1$ set starting values for $d^k = d_0$, $\bar{r}^k = r_0$.
2. Initialize Λ_j at the posterior mode conditional on d^k and \bar{r}^k .
3. Draw Λ_j^k according to steps 2 and 3 from the algorithm in the previous section.
4. Draw $\Sigma_j^k | d^k, \bar{r}^k, \Lambda_j^k, y_j$, and $\beta_j^k | d, \bar{r}^k, \Lambda_j^k, \Sigma_j^k, y_j$ from their posteriors given by (22).
5. Draw a candidate value for r^* by: $r^* = \bar{r}^{k-1} + \Phi \epsilon$ with: $\epsilon \sim N(0, 1)$ and Φ is a scaling factor ensuring an acceptance rate of about 20%.
6. Accept the draw with probability

$$p^k = \min \left\{ 1, \frac{p(Y_t | r^*, \theta)}{p(Y_t | \bar{r}^{k-1}, \theta)} \right\} \quad (5)$$

where $p(\cdot)$ denotes the posterior density given all other parameters of the model.

7. Draw d from

$$p(d=i | Y_t, \theta) = \frac{p(Y_t | d, \theta)}{\sum_{d=1}^{d_0} p(Y_t | d, \theta)} \quad \text{for: } i = 1, \dots, d_{\max}. \quad (6)$$

8. Generate $e_{j,T+1}, \dots, e_{j,T+h}$ from $\epsilon_{j,t} \sim N(0, \Sigma_j^k)$ and compute h -step-ahead forecasts recursively by iterating (2) and (3) h periods into the future.
9. Redo until $k = D + R$.

I employ 25000 iterations of the Gibbs sampler and discard the first 20000 as burn-ins.

The key element of this model is the threshold variable r , which governs the regime dependency. Different specifications for r are proposed in the literature. Caggiano *et al.* (2014) and Caggiano, Castelnovo and Figueres (2017) argue that recessions are particularly informative regarding the identification of uncertainty shocks. These studies follow Auerbach and Gorodnichenko (2012) and use a moving average of GDP growth rates as threshold variable. Other

studies emphasize the importance of the uncertainty proxy itself and condition on either the historic change (for example, Henzel and Rengel, 2017; Foerster, 2014) or the historic level of the uncertainty proxy (Jones and Enders, 2016; Berg, 2017a; Castelnuovo and Pellegrino, 2018, among others). Since this paper aims at identifying uncertainty regimes, I follow the latter and specify r as the level of the uncertainty indicator.

However, nowadays there are various uncertainty proxies available, for example, stock market volatility (Bloom, 2009), newspaper-based indices (Baker, Bloom and Davis, 2016), firm-level data-based indices (Bachmann, Elstner and Sims, 2013), indices based on macroeconomic forecast errors (Rossi and Sekhposyan, 2015), and indices based on the residuals from factor augmented regressions (Jurado *et al.*, 2015). I choose the macroeconomic uncertainty index provided by Jurado *et al.* (2015), a choice motivated by two factors. First, this proxy defines uncertainty in terms of the variation in the unforecastable component of macroeconomic variables and not in terms of the variables' raw volatility.⁴ Second, and in contrast to other measures, it is based on a large number of economic indicators and, hence, should represent an aggregate uncertainty factor that affects many series, sectors, or markets (Jurado *et al.*, 2015).⁵

I recursively construct the index to avoid that the index at a given point in time includes information that would not be available to the forecaster at this moment. As already pointed out by Jurado *et al.* (2015), the indices based on both in-sample forecasts and out-of-sample forecasts are highly correlated.

3 Data and Forecast Methodology

The dataset includes 11 quarterly US macroeconomic series from 1960Q3 through 2017Q4 covering a broad range of economic activity especially relevant for policymakers and central bankers.⁶ The series are obtained via the Federal Reserve Economic Database (FRED). To study the impact of macroeconomic uncertainty on the forecast performance, I further augment the dataset with the economic uncertainty index developed by Jurado *et al.* (2015).

Most of the series enter the model in annualized log levels, that is, I take logarithms and multiply by 4, except for those series that are already expressed as annualized rates. For the stationary variables, I utilize a white noise prior ($\delta_i = 0$), whereas for integrated series a random walk prior ($\delta_i = 1$) is used. A detailed description of the data, their corresponding transformations and sources is provided in Table 1. For both models, I generate 1- up to 4-quarter-ahead forecasts by a recursive estimation scheme over an expanding window. The initial sample runs from 1960Q3 to 2004Q3. Thus, I generate forecasts for 2004Q4 until 2005Q3 in the first recursion. Subsequently, I iterated the procedure by updating the estimation sample with the observations from the next quarter until 2016Q4 is reached. This procedure generates a total of 50 forecasts

⁴The unforecastable component is defined as the expected squared forecast error of a series conditional on all available information.

⁵The macroeconomic uncertainty index is based on the FRED-MD database provided by McCracken and Ng (2016), which consist of 134 series representing broad classes of variables.

⁶Although a large Bayesian VAR is, in general, capable of processing a much higher number of economic indicators, even medium-sized BVARs produce accurate forecasts (see, for example, Bańbura *et al.*, 2010; Koop, 2013; Berg, 2016).

for each horizon. Forecasts for horizons larger than one are obtained iteratively. The lag length in all VARs is set to four. While I estimate the model with both stationary and integrated variables, I report results solely in terms of annualized percentage growth rates. To this end, I transform the models' level forecasts for the integrated variables into growth rates based on these level forecasts.

Table 1: Dataset

Variable	Mnemonic	Source	Transformation
Real GDP	GDPC1	FRED	$\log \times 400$
CPI for All Urban Consumers: All Items	CPIAUCSL	FRED	$\log \times 400$
Industrial Production Index	INDPRO	FRED	$\log \times 400$
All Employees: Total Nonfarm	PAYEMS	FRED	$\log \times 400$
Civilian Unemployment Rate	UNRATE	FRED	–
Real Gross Private Domestic Investment	GPDIC1	FRED	$\log \times 400$
ISM Manufacturing: PMI Composite Index	NAPM	FRED	–
Personal Consumption Expenditures, Price Index	PCECTPI	FRED	$\log \times 400$
Capacity Utilization: Total Industry	TCU	FRED	–
Federal Funds Rate	FEDFUNDS	FRED	–
S&P 500 Composite - Price Index	S&PCOMP	FRED	$\log \times 100$
Macroeconomic Uncertainty Index	–	own calculations	–

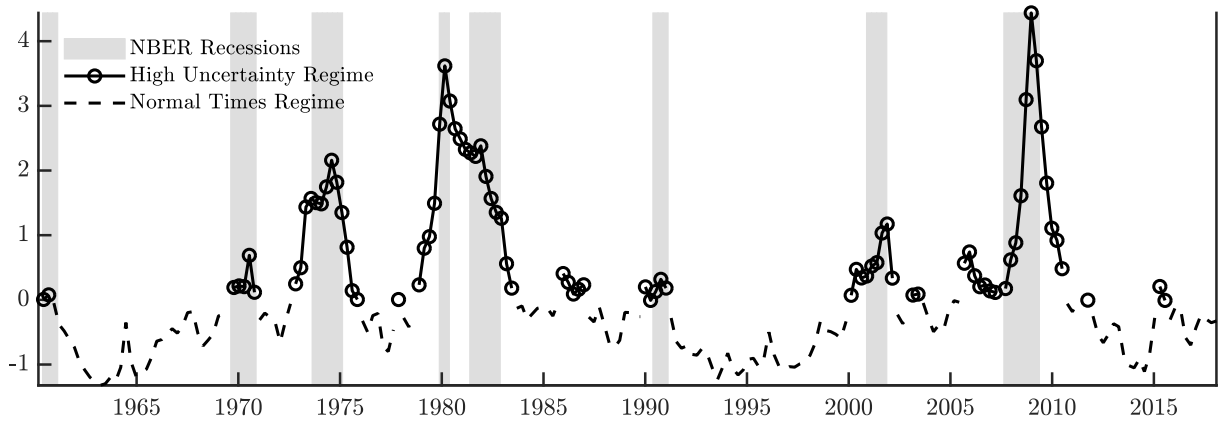
Notes: The macroeconomic uncertainty index is calculated using the codes provided by Jurado *et al.* (2015) modified to provide a recursively estimated index.

4 In-Sample Analysis

Now that we have outlined the empirical setup, we turn to investigating the in-sample properties of the Bayesian threshold VAR, which are based on full-sample estimates. Figure 1 plots the macroeconomic uncertainty index along with NBER recessions. The solid-dotted line refers to the episodes of the endogenously identified high uncertainty regime, while the dashed line corresponds to the normal times regime. The figure reflects the common knowledge that macroeconomic uncertainty is countercyclical. Moreover, while the uncertainty regimes partly coincide with NBER recessions, they are more persistent and more frequently identified.⁷ These discrepancies can be explained by differences in the concepts. NBER defines recessions as significant decline in economic activity, whereas the macroeconomic uncertainty index focuses on predictability. Obviously, the latter implies that booms and recoveries, which are characterized by high growth rates of macroeconomic aggregates, are excluded from the NBER recessions but can be part of the high uncertainty regime if the evolution of these aggregates is hard to predict during these episodes. Nevertheless, these results suggest that recessions are a useful proxy for uncertainty regimes. To directly identify regimes based on the prevailing level of uncertainty, however, might be more appropriate for capturing possible nonlinear dynamics.

⁷For example, according to the NBER Business Cycle Dating Committee, the recession induced by the burst of the dot-com bubble lasted for the entire year 2001, while the high uncertainty regime in turn starts in the first quarter of 2000 and lasts until the first quarter of 2002. The same holds for the Great Recession, which is dated from 2008Q1 until 2009Q2 according to the NBER. The high uncertainty regime begins already in 2007Q2 and then lasts until 2010Q2.

Figure 1: Estimated Uncertainty Regimes



Note: Shaded areas correspond NBER recessions. Dashed-dotted line refers to the high uncertainty regime, i.e. the median estimate of $(1-S_t)$ from (2) and (3).

Having identified uncertainty regimes, we assess whether uncertainty has different effects on the economy depending on the prevailing regime. For this purpose, we perform a structural analysis based on impulse responses.⁸ As the threshold VAR from Section 2.2 is nonlinear, standard impulse responses are not appropriate for capturing the effects of a shock. Thus, I follow Koop *et al.* (1996) and compute generalized impulse responses (GIRFs). Formally, the GIRF at horizon h of variable y to a shock of size ϵ and conditional on an initial condition I_{t-1} is defined as the difference between two conditional expectations:

$$\text{GIRF}_y(h, \epsilon, I_{t-1}) = E[y_{t+h}|\epsilon, I_{t-1}] - E[y_{t+h}|I_{t-1}], \quad (7)$$

where the terms on the right-hand side are approximated by a stochastic simulation of the model. I calculate for each initial condition 500 time paths of length h each with an uncertainty shock hitting the system in the initial period and without this shock. I then average across the differences between both time paths to obtain the GIRF for the respective history. To compute regime-dependent responses, I average over the GIRFs based on the histories of the normal times and high uncertainty regime, respectively. Moreover, I follow Kilian and Vigfusson (2011) and consider orthogonalized residuals to identify uncertainty shocks. The shocks are identified using a recursive estimation scheme based on a Cholesky decomposition with uncertainty ordered second and the S&P 500 ordered first. The latter allows real and nominal variables to react instantaneously to an uncertainty shock (see Bloom, 2009; Fernández-Villaverde *et al.*, 2015; Baker *et al.*, 2016, among others). Since the T-VAR captures regime-dependent shock sizes and shock propagation processes, I consider both a one standard deviation shock and a unit shock to assess whether differences in the responses are triggered by the size of the shock or by its propagation. Due to space constraints, I only present the results for GDP, GDP deflator,

⁸For generating the impulse responses, the variables enter the model in logarithms multiplied by 100 so that they can be interpreted as percentage deviations from the trend. Moreover, the macroeconomic uncertainty index is standardized to facilitate the interpretation of the shock sizes.

investment, consumption, the unemployment rate, and the federal funds rate.⁹ The left column of Figure 2 plots the responses to a one standard deviation uncertainty shock that is different in magnitude across the regimes. The right column depicts the responses for the unit shock. The red line is the response in the high uncertainty regime; the blue line corresponds to the normal times regime. Shaded areas and dashed lines refer to 68% error bands.

First, Figure 2 shows that independently of both the size of the shock and the regime, an increase in macroeconomic uncertainty operates as a negative demand shock. Private consumption drops persistently. A likely explanation for this is precautionary saving by households. The latter reduces the demand for investment goods and leads to a decline in investment, which is roughly twice as large as the drop in consumption. Moreover, the responses point at the existence of the real option effect. As a consequence of increased uncertainty, investors postpone investment decisions – if investment is (partially) irreversible – until business conditions become clearer (Bernanke, 1983). Finally, the unemployment rate persistently increases and follows a hump-shaped path with a peak effect occurring seven quarters subsequent to the impact period. These results are in line with previous studies (see, for instance, Caggiano *et al.*, 2014; Caldara *et al.*, 2016) and follow the predictions of theoretical models incorporating price rigidities (Basu and Bundick, 2017; Bonciani and van Roye, 2016).

Evidence regarding the price response to an increase in uncertainty is mixed. Figure 2 depicts weak inflationary effects and supports the findings of Alessandri and Mumtaz (2018), Mumtaz and Theodoridis (2015, 2018), and Popescu and Smets (2010). Other studies stress the deflationary effects of uncertainty shocks (see, for instance, Christiano *et al.*, 2014; Leduc and Liu, 2016; Carriero *et al.*, 2015). From a theoretical point of view, the responses provide evidence in favor of an “inverse Oi (1961)-Hartman (1972)-Abel (1973) effect”. As pointed out by Born and Pfeifer (2014, 2017) and Fernández-Villaverde *et al.* (2015), given sticky prices, firms can set a price, which is either too low or too high. The former is obviously not optimal because the firm has to sell too many units at a too low price. However, in the latter case, the firm sells too few units but is compensated by a higher price per unit. Therefore, firms are prone to an upward bias in future prices, which can lead to inflationary effects of an uncertainty shock.

Second, the estimated size of the uncertainty shock is roughly 1.5 times larger in the high uncertainty regime than in the normal times regime (0.22 to 0.33). However, the persistence of the shock is significantly lower in the high uncertainty regime. Third, comparing the responses across regimes reveals statistically significant differences. The impact of the shock is much larger during times of high uncertainty. Investment, for instance, drops by roughly 0.5% in normal times compared with a decline by 2.0% in times of high uncertainty. The same pattern holds for the unemployment rate, which significantly increases to roughly twice as high in the high uncertainty regime (0.35% versus 0.17%). Thus, in line with previous studies, the contractionary effects of uncertainty shocks are especially large when uncertainty is already at a high level (Jones and Enders, 2016; Bijsterbosch and Guérin, 2013). These results suggest that using a linear model potentially underestimates the actual effect of a sudden hike in economic uncertainty. Finally, as in Caggiano *et al.* (2014) and Alessandri and Mumtaz (2018), monetary policy seems to react

⁹The effects for the remaining variables are presented in Appendix C.

to uncertainty shocks only in crisis periods (either recessions or financial stress) by lowering the policy rate. However, the response is not distinguishable from zero.¹⁰

To arrive at a better impression of the relative importance of the shock's size and its propagation, Figure 3 depicts the differences in the responses between both regimes along with 68% error bands. Overall, the differences in the responses to the unit shock are larger, however, the corresponding error bands are wide and differences become insignificant after a few quarters for most variables. In contrast, the differences between the state-dependent responses of the one standard deviation shock are less pronounced but remain significantly different from zero longer. This suggests that the shock size is a very important factor for the state-dependency of the responses. From a forecasting perspective, this might yield more accurate density forecasts, since the nonlinear model is potentially better at capturing the state-dependent disturbances.

5 Forecast Evaluation

In this section, the forecasts of the competing models are evaluated. I first discuss the measures used for the evaluation of both point forecasts and the predictive densities. Subsequently, the forecast performance is highlighted. In the following, j , i , and h denote the model, variable, and forecast horizon, respectively, for the forecast sample $t = 1 \dots, N$.

5.1 Forecast Metrics

A first impression of the models' forecast performance is provided by the mean forecast error (MFE), which indicates the average deviation of the forecast from the realization. Thus, positive (negative) MFEs show that the model on average overestimates (underestimates) the true value. The MFE is defined as follows:

$$\text{MFE}_{i,j}^h = \frac{1}{N} \sum_{T=T_0+h} (\bar{y}_{i,T|T-h}^j - y_{i,T}), \quad (8)$$

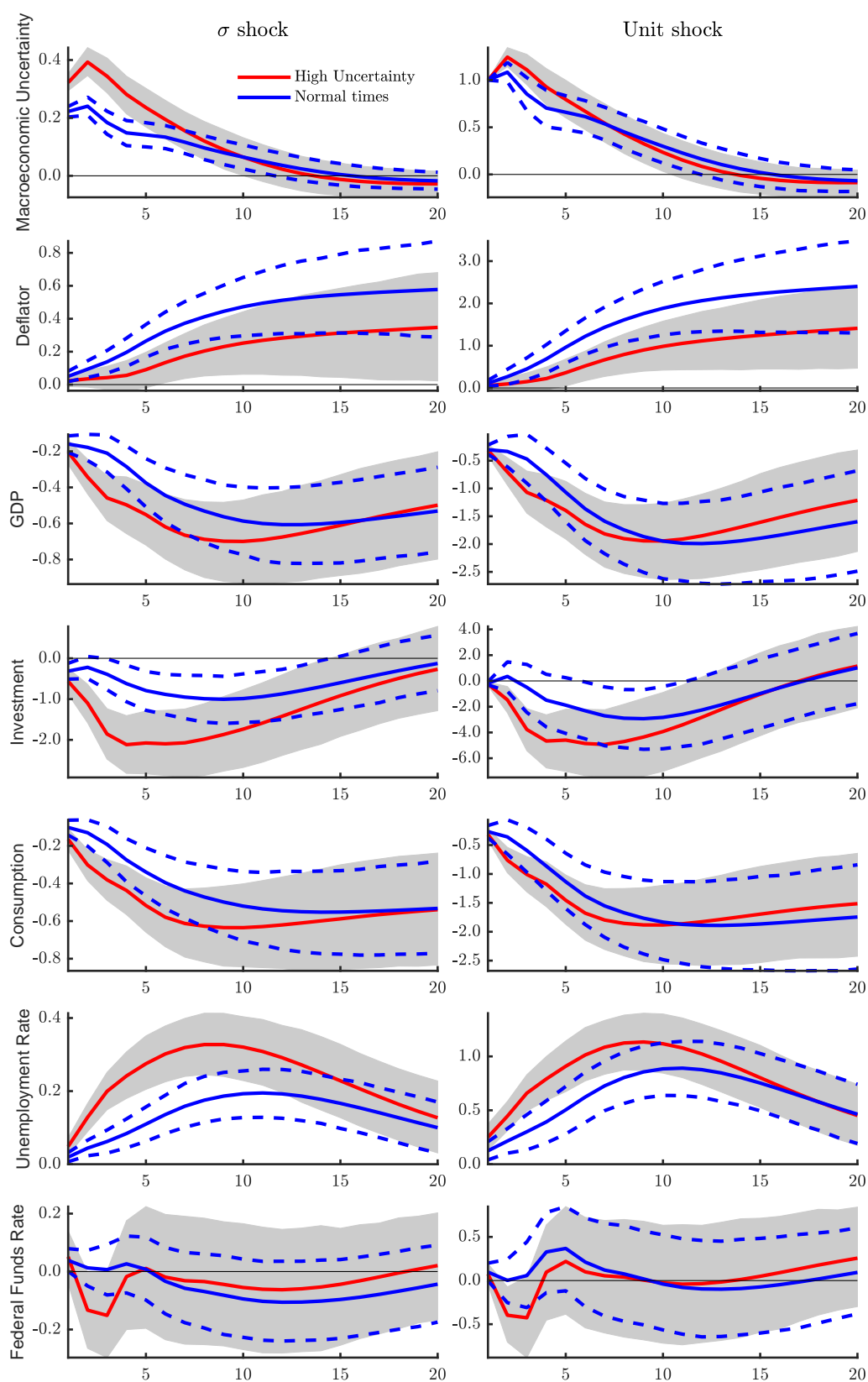
where $\bar{y}_{i,T|T-h}^j$ and $y_{i,T}$ denote the mean of the model's predictive density and the corresponding realization. The MFE is informative on its own and facilitates an absolute evaluation of the point forecast accuracy. However, since positive and negative errors cancel each other out according to the MFE, I further evaluate point forecasts in terms of the root mean squared forecast error (RMSFE):

$$\text{RMSFE}_{i,j}^h = \sqrt{\frac{1}{N} \sum (\bar{y}_{i,T|T-h}^j - y_{i,T})^2}. \quad (9)$$

While the MFE can be interpreted on its own, the RMSFE is only useful in assessing the accuracy of a model compared to that of other models. Therefore, I report the RMSFEs relative

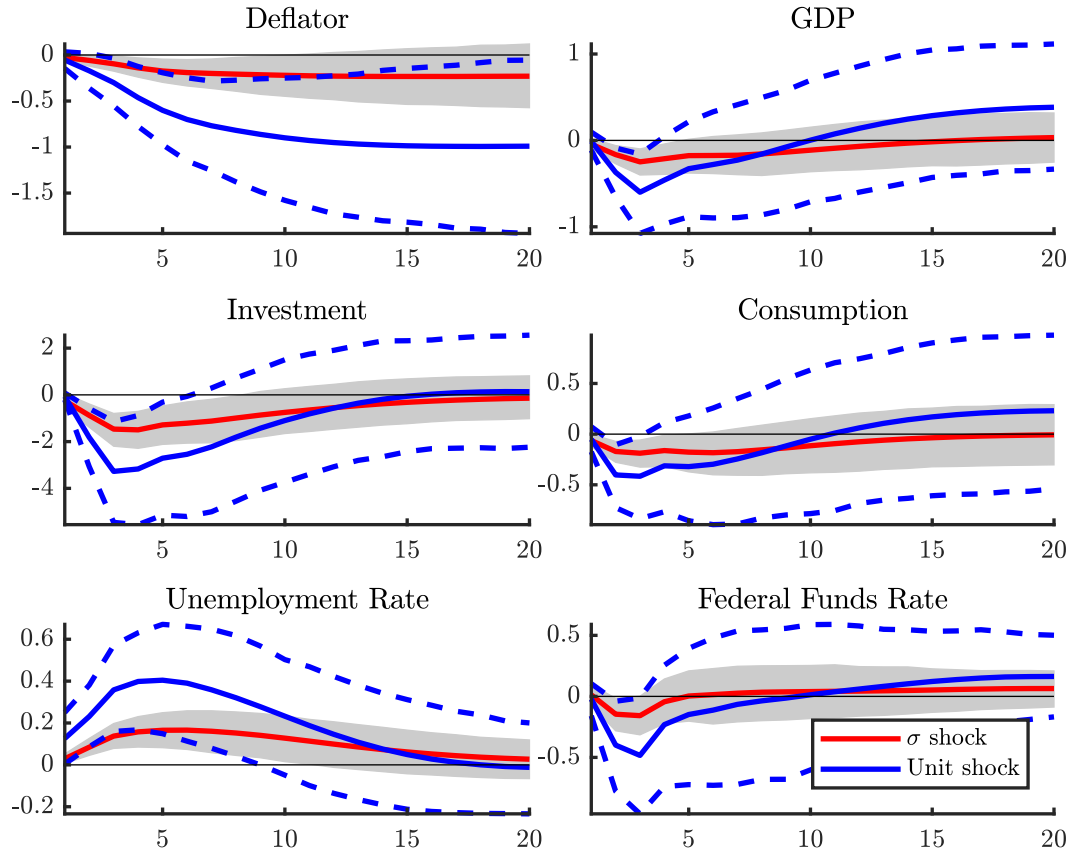
¹⁰The interest rate response documented by Caggiano *et al.* (2014) is somewhat larger. The latter analysis, however, does not allow for regime switches in the responses, which tends to increase the effect of a shock.

Figure 2: Generalized Impulse Responses to an Uncertainty Shock



Note: The figure displays the impact of an uncertainty shock to selected variables in normal times and in times of high uncertainty. The left column refers to a one standard deviation innovation; the right column depicts a unit shock. The responses are generated using a recursive identification scheme with uncertainty ordered second. Gray shaded areas and dashed blue lines refer to 68% error bands. The macro uncertainty index enters the model standardized.

Figure 3: Differences in Generalized Impulse Responses Between Normal times and High Uncertainty Regime



Note: The figure displays the differences in the responses between high uncertainty and normal times for a one standard deviation shock (red line) and a unit shock (blue line). Gray shaded areas and dashed blue lines refer to 68% error bands.

to a benchmark model:

$$\text{relative RMSFE}_{i,j}^h = \text{RMSFE}_{i,j}^h / \text{RMSFE}_{i,B}^h, \quad (10)$$

where $\text{RMSFE}_{i,h}^B$ refers to the RMSFE of the benchmark model, which is the linear VAR from Section 2.1 without employing the macro uncertainty indicator. To test whether the forecasts are significantly different from each other, I apply the test provided by Diebold and Mariano (1995) adjusted for the small-sample correction of Harvey, Leybourne and Newbold (1997).

For a long time, the evaluation of economic forecasts focused solely on point forecasts, but in the recent past, the uncertainty around the forecasts has become an important issue. To take into account this uncertainty, additionally I evaluate the predictive densities. I assess the accuracy of the densities by means of scoring rules. The latter concept is based on the idea of comparing the quality of probabilistic forecasts by assigning a numerical value via the predictive distribution and a realization of the predicted value. Specifically, I apply the average log predictive score, which goes back to Good (1952) and has become a commonly accepted tool for comparing the forecast performance of different models (see Geweke and Amisano, 2010; Clark, 2012; Jore, Mitchell and

Vahey, 2010, among others).¹¹ It is defined as the logarithm of the predictive density evaluated at the realized value:

$$LS_{i,j}^h = \frac{1}{N} \sum_{\log} p_t(y_{i,t+h}|j). \quad (11)$$

The predictive density, $p(y_{t+h}|j)$, is obtained by applying a kernel estimator on the forecast sample.¹² Hence, if the competing model has a lower log score than the benchmark, its forecasts are closer to the realizations with a higher probability. As for the RMSFE, the log scores are not informative on their own, which is why I report them relative to the benchmark model ($LS_{B,i}^h$):

$$\text{relative } LS_{i,j}^h = LS_{i,j}^h - LS_{i,B}^h. \quad (12)$$

Furthermore, I evaluate the predictive densities in terms of the (average) continuous ranked probability score (CRPS) introduced by Matheson and Winkler (1976). The latter measures the integrated squared difference between the cumulative predictive distribution function, $P(\cdot)$, and the associated cumulative distribution function of the realization and thus corresponds to the MAFE in case of density forecast evaluation. As argued by, for instance, Gneiting and Raftery (2007), the CRPS has two advantages compared to the log scores. First, it can be reported in the same units as the respective variable and therefore facilitates a direct comparison of deterministic and probabilistic forecasts. Second, in contrast to log scores, CRPSs are both less sensitive to extreme outcomes and better able to assess forecasts close but not equal to the realization. I follow Gneiting and Ranjan (2011) and express the CRPS in terms of a score function:

$$S(p, y_{i,t+h}, \nu(\alpha)) = \int_{-0}^1 QS_{\alpha}(P(\alpha)^{-1}, y_{i,t+h}) \nu(\alpha) d\alpha, \quad (13)$$

where $QS_{\alpha}(P_t(\alpha)^{-1}, y_{i,t+h}) = 2(I\{y_{i,t+h} < P_t(\alpha)^{-1}\} - \alpha)(P_t(\alpha)^{-1} - y_{i,t+h})$ is the quantile score for forecast quantile $P_t(\alpha)^{-1}$ at level $0 < \alpha < 1$. $I\{y_{i,t+h} < P_t(\alpha)^{-1}\}$ is an indicator function taking the value one if $y_{i,t+h} < P_t(\alpha)^{-1}$ and zero otherwise. $\nu(\alpha)$ is a weighting function. Applying a uniform weighting scheme, yields the average CRPS:

$$CRPS_{i,j}^h = S(p_t, y_{i,t+h}, 1). \quad (14)$$

To compute this expression, $P(\cdot)$ is approximated by the empirical distribution of forecasts and the integral is calculated numerically.¹³ According to this definition, lower CRPSs imply that the predictive density is more closely distributed to the actual density. As for the log scores, I report the CRPS in terms of the average across all evaluation periods and relative to the benchmark model. To provide a rough gauge on whether these scores are significantly different from the benchmark, I follow D'Agostino, Gambetti and Giannone (2013) by regressing the differences

¹¹A survey concerning alternative scoring rules is provided by Gneiting and Raftery (2007).

¹²Since the predictive density is not necessarily Gaussian, I do not resort to the frequently used approximation of Adolfson, Lindé and Villani (2007).

¹³As shown by Smith and Vahey (2015), this procedure is more accurate than expressing the CRPS as the difference of two expectations and the approximation of these expectations using Monte Carlo draws (see Gneiting and Raftery, 2007; Panagiotelis and Smith, 2008).

between the scores of each model and the benchmark on a constant. A t-test with Newey-West standard errors on the constant indicates whether these average differences are significantly different from zero.

Finally, I compute probability integral transforms (PITs) developed by Rosenblatt (1952) and popularized in economics by Diebold, Gunther and Tay (1998). The PIT is defined as the CDF corresponding to the predictive density evaluated at the respective realizations:

$$z_{t+h}^i = \int_{-\infty}^{y_{t+h}^i} p_t(u) du \quad \text{for } t = 1, \dots, N. \quad (15)$$

Thus, with regard to the respective predictive density, the PIT denotes the probability that a forecast is less or equal to the realization. For example, a realization that corresponds to the 10th percentile receives a PIT of 0.1. Hence, if the predictive densities match the true densities, the PITs are uniformly distributed over the unit interval. To assess the accuracy of the predictive density according to the PIT, it is convenient to divide the unit interval into k equally sized bins and count the number of PITs in each bin. If the predictive density equals the actual density, each bin contains N/k observations. In the following, I set $k = 10$, implying that each bin accounts for 10% of the probability mass. Moreover, I follow Rossi and Sekhposyan (2014) and compute 90% confidence bands by using a normal approximation to gauge significant deviation from uniformity.

5.2 Point Forecasts

Table 2 summarizes the results of the forecast evaluation based on MFEs and RMSFEs. The dimension for measures is percentage points. While the models provide forecasts for each variable in the dataset, for the sake of brevity, I present results only for the variables depicted in Section 4, namely, inflation (measured in terms of the GDP deflator growth), GDP growth, consumption growth, investment growth, the unemployment rate, and the federal funds rate.¹⁴ Let us begin by analyzing the results for MFE presented in the left panel of Table 2. The table shows that the benchmark VAR on average and in most cases overestimates the realization. Inflation for the next quarter, for instance, is overpredicted by 0.14 annualized percentage points. Adding the uncertainty index to the otherwise standard VAR (VAR^U) tends to increase this bias except for the unemployment rate and for investment growth. In the latter case, the MFE is on average over all horizons about one percentage point smaller. The MFEs of the threshold VAR (T-VAR) are distinct from the former ones. First, compared to the linear models, the MFEs from the T-VAR are in most cases larger. Only for certain variables and horizons (for example, output growth at $h=3$) reductions are detectable. Thus, identifying uncertainty regimes seems to be less fruitful for generating well-calibrated predictive means. Second, while the linear models consistently underpredict unemployment and overpredict the federal funds rate, the T-VAR overpredicts unemployment and underpredicts the federal funds rate. The latter result stems from the fact that the T-VAR predicts federal funds rate values below zero even though the federal funds rate

¹⁴Results for the remaining variables are available upon request.

is fixed at its lower bound.¹⁵ Overall, the evaluation of the MFEs, thus, provides only little evidence in favor of both the VAR^U and the T-VAR. In fact, the benchmark model provides very competitive MFEs and in some cases outperforms the remaining models.

The right panel of Table 2 depicts the results for the RMSFE. With respect to the benchmark model, the RMSFEs are reported in absolute terms, while the remaining specifications are reported as ratios relative to the benchmark model, i.e. a figure below unity indicates that the model outperforms the benchmark specification. The differences between the VAR and the VAR^U are again very small and in most cases insignificant, suggesting that the uncertainty index has on average only marginal impact on the forecast performance in a linear setting. Only for the federal funds rate, the VAR^U provides significantly smaller RMSFEs. The results for the threshold VAR are mixed. In most cases, the latter is outperformed by its linear counterparts, implying that identifying uncertainty regimes is not beneficial with regard to point forecasting. The worst relative performance is obtained for inflation forecasts. Moreover, neither for GDP growth, nor for investment or consumption growth, the T-VAR delivers a reduction in RMSFEs. While for the former indicators regime-dependency apparently does not pay off, unemployment and interest rate forecasts benefit significantly. Regarding the federal funds rate at the one and two-quarter ahead horizons, the T-VAR's forecasts are on average 14% and 8% more precise, respectively, while with regard to the unemployment rate forecast, accuracy increased by 6% and 7% for these horizons. These results are particularly appealing since labor market variables possess an especially strong regime dependency with regard to uncertainty (see Figures 2 and 3). In addition, these findings underpin the results of Barnett *et al.* (2014) and Alessandri and Mumtaz (2017). While the former demonstrates that regime-dependent VARs are inferior to linear VARs and VARs with time-varying parameters with regard to GDP growth and inflation, the latter provides evidence that financial variables particularly benefit from regime dependency. Thus, it is suggested that for activity variables there is, if any, only gradual structural change, which cannot be covered by a threshold VAR, while for labor market and financial variables the structural shift is more abrupt and thus can be captured by the T-VAR.

Figure 4 explores the models' forecast performance over time. To this end, I calculate four-quarter moving averages of the MFE (upper panel) and relative RMSFE (lower panel) for one-quarter-ahead forecasts of the unemployment rate (left column) and federal funds rate (right column). Evidently, the degree of predictability varies substantially over time. Regarding unemployment rate forecasts, the VAR^U and the T-VAR work particularly well during the Great Recession and the subsequent recovery when uncertainty was high. In the remaining periods, when uncertainty was rather low, the forecast performance is very similar (VAR^U) or even worse (T-VAR) compared to the linear VAR, suggesting that uncertainty is especially relevant when it is high. A similar pattern arises for the federal funds rate. The largest gains in forecast accuracy are obtained during 2008–2012 when uncertainty was high. However, in contrast to the unemployment rate, federal funds rate forecasts are also more precise from 2013–2016, while the short hike of the federal funds rate in 2012 is captured best by the linear VAR; both the VAR^U and the T-VAR strongly overestimate the actual increase. Overall, the results suggest that including

¹⁵Berg (2017b) studies how this issue affects the forecast performance of linear VARs.

Table 2: MFEs and RMSEs

Specification	MFE				RMSFE			
	$h = 1$	$h = 2$	$h = 3$	$h = 4$	$h = 1$	$h = 2$	$h = 3$	$h = 4$
Inflation								
VAR	0.14	0.17	0.18	0.18	0.95	1.02	1.09	1.15
VAR ^U	0.16	0.21	0.25	0.27	1.10	1.06	1.02•	1.04
T-VAR	0.35	-0.34	-0.84●	1.20●	1.19●	1.08	1.28●	1.45●
Output growth								
VAR	0.97●	1.11●	1.15●	1.00●	2.35	2.79	2.91	2.80
VAR ^U	1.14●	1.16●	1.25●	1.15●	1.06•	1.03	1.01	0.99
T-VAR	1.39●	0.77	-0.05	0.79	1.17●	1.04	0.92	0.97
Investment growth								
VAR	4.30●	5.44●	5.65●	4.48●	10.27	15.01	15.52	13.76
VAR ^U	3.36●	4.00●	4.64●	3.83●	0.96	0.99	1.03	0.97
T-VAR	4.88●	0.55	-5.11●	-4.42●	1.18●	0.92	1.00	1.06
Consumption growth								
VAR	0.77●	0.72●	0.73●	0.87●	2.14	2.13	2.08	2.34
VAR ^U	0.77●	0.74●	0.82●	0.95●	1.01	0.98	1.03	0.97
T-VAR	1.11●	1.00●	0.86	2.07●	1.12●	1.19●	1.11	1.30●
Unemployment rate								
VAR	-0.04	-0.09	-0.15	-0.20	0.22	0.47	0.73	1.00
VAR ^U	-0.03	-0.06	-0.11	-0.16	1.01	0.97	0.97	0.96
T-VAR	-0.03	0.08	0.29●	0.50●	0.94•	0.93•	1.06	1.13●
Federal funds rate								
VAR	0.01	0.09	0.17	0.27	0.65	1.16	1.42	1.58
VAR ^U	0.08	0.19	0.29●	0.40●	0.90•	0.98	1.06	1.14●
T-VAR	0.04	-0.24	-0.51●	-0.71●	0.86●	0.92•	1.04	1.16●

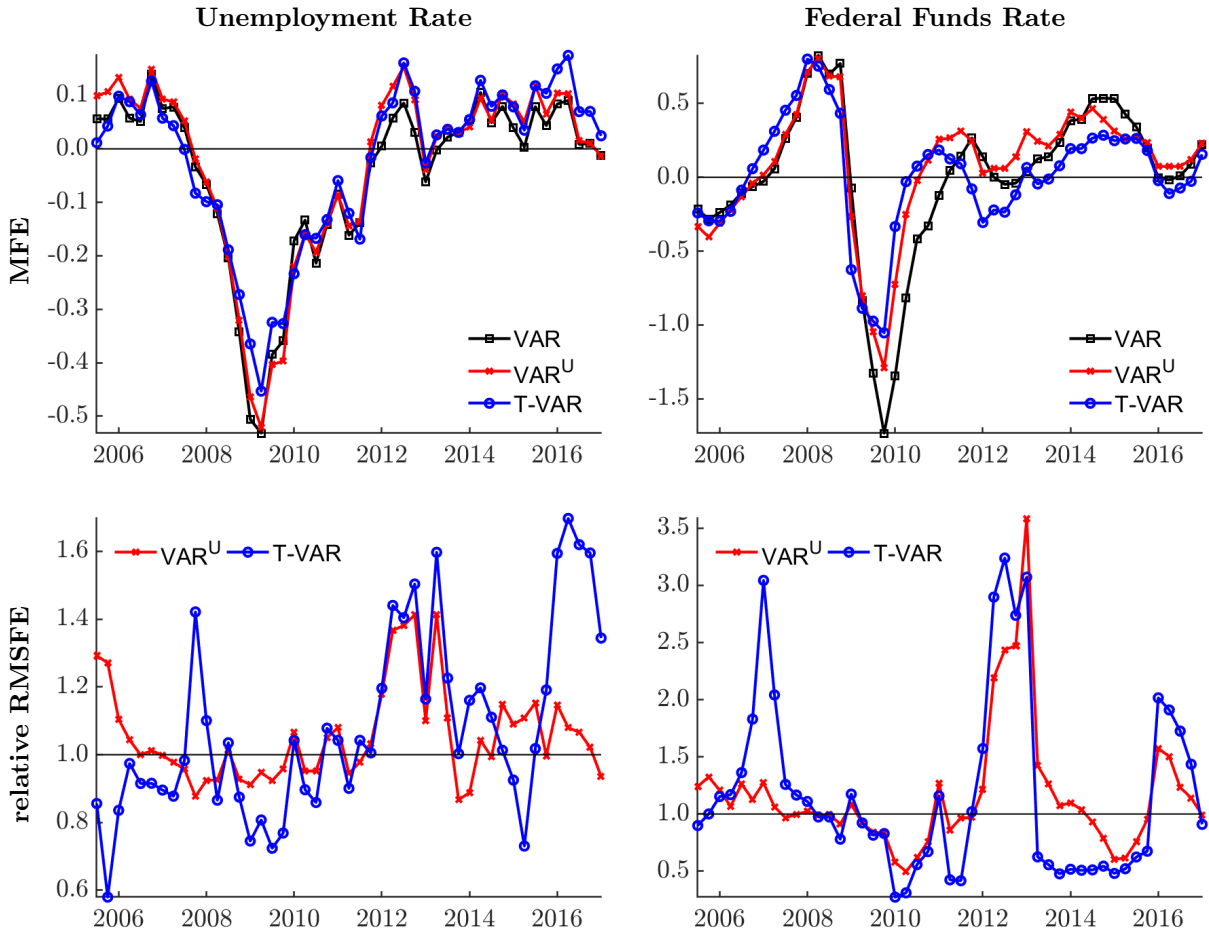
Notes: VAR and VAR^U denote the linear VAR both without macro uncertainty and including macro uncertainty, respectively. T-VAR refers to the threshold VARs. RMSFEs are reported in absolute terms for the benchmark model and in ratios relative to the benchmark for the remaining specifications. Ratios below unity indicate that the model outperforms the benchmark. ●, •, and • denote that the errors are significantly different from zero (MFE) or the benchmark (RMSFE) on the 5%, 10%, and 15% level, respectively. Sample: 1960Q3–2017Q4.

information on economic uncertainty can improve point forecast accuracy for some variables and for short horizons, with the largest gains during episodes of high uncertainty.

5.3 Density Forecasts

Subsequently, we evaluate the models' forecasts with respect to the predictive densities. Thus, apart from the predictive mean evaluated above, the variances have to be precisely estimated as well to ensure an accurate predictive density. Table 3 sets out the results for the CRPS and the LS. First, we consider the results for the LS, which are reported in levels for the benchmark

Figure 4: Forecast Performance Over Time – Point Forecasts



Note: The figure displays mean forecast errors (upper panel) and relative root mean squared forecast errors (bottom panel) computed as a four-quarter moving average over the forecast sample for unemployment and federal funds rate forecasts.

and in differences for the remaining models. Positive differences indicate that the respective model outperforms the benchmark. With regard to the linear models, the LS provide a pattern similar to that in the previous section. Again, the differences between both models are rather small, indicating that the marginal impact of the uncertainty index in a linear setting is on average almost negligible. However, in some cases, already the linear VAR using additional information on economic uncertainty provides significantly better (lower) LS. Turning to the T-VAR reveals that for medium- to long-term forecasts, controlling for regime-dependency with respect to uncertainty leads to considerably less accurate predictive densities. Regarding short-term forecasts, though, the T-VAR provides, for most variables, remarkably better log scores, with the largest improvements obtained for the activity variables. For instance, the LS for output growth at $h = 1$ is 19% lower than the benchmark's score. Hence, while the T-VAR is inferior in generating precise point forecasts for the activity variables, it is superior in computing the complete predictive distribution of these indicators and thus is better suited for describing the uncertainty around the point estimate.

In total, the CRPS underpin the findings of the LS. However, there are noteworthy differences

in regard to the unemployment rate. While according to the LS the predictive distributions of the T-VAR are virtually identical to the ones of the benchmark, according to the CRPS, the T-VAR provides significantly more accurate densities. For instance, the one-quarter-ahead CRPS for the unemployment rate is 16% lower than the benchmark's CRPS while the average log score is virtually identical. The latter suggests that the log scores regarding the unemployment forecasts are partly distorted by outliers. Overall, the evaluation of both the LS and CRPS underpins findings of previous studies demonstrating that nonlinearity is particularly useful in calibrating accurate predictive densities (see Chiu, Mumtaz and Pintér, 2017; Huber, 2016; Groen, Paap and Ravazzolo, 2013, among others). However, while the former studies mainly focus on forecasting output, inflation, and interest rates, this paper shows that unemployment rate forecasts also benefit significantly. Figure 5 presents evidence on time-varying predictability. Similar to Figure 4, the T-VAR provides more accurate densities during the Great Recession and the subsequent recovery.

Between 2011 and the end of 2013, the T-VAR's entire forecast distribution is stretched by a few forecasts far away from the realizations, which leads to low log scores. Since the CRPS is better able to reward the observations close to the realization and is more robust to outliers, according to the CRPS, the T-VAR provides more precise densities even for this period and thus for almost the entire evaluation period. For the federal funds rate, the picture is more clear-cut. The LS indicate that the T-VAR is superior at the beginning of the Great Recession, but the CRPS display more accurate predictive densities for almost the entire sample. As for the unemployment rate, the T-VAR provides the best relative forecast performance during the Great Recession and the subsequent recovery when economic uncertainty was very high. In total, Figure 5 provides evidence for important changes in the predictive ability of the models.

Finally, I compute PITs to gauge the calibration of the predictive densities. Figure 6 facilitates a graphical inspection of the PITs and shows that the predictive densities look similar for the different models.¹⁶ As I computed 50 forecasts for each horizon, each bin in Figure 6 should contain five observations (depicted by the solid black line) to ensure uniformity. Thus, the closer the histograms are to the solid black line, the more accurate are the predictive densities. In case of inflation, output, investment, and consumption, the PITs appear hump-shaped, with significant departures from uniformity. In fact, the models assign too much probability to the center of the distribution with too many PIT-values around 0.5. The latter indicates that the kurtosis of predictive densities at each horizon and recursion is higher than the kurtosis of true density, which implies that the models overestimate the actual uncertainty around the point estimate. This pattern is frequently found in the VAR forecasting literature – see, for example, Rossi and Sekhposyan (2014), Bekiros and Paccagnini (2015) or Gerard and Nimark (2008) – and can be caused by a too dense parametrization of the model.¹⁷ With regard to one-quarter-ahead forecasts (blue bars), the T-VAR mitigates this issue by generating more forecasts that correspond to the lower percentiles of the actual distribution and thus provides a better description of the

¹⁶Alternatively, one can also pursue more formal approaches to evaluate PITs; see, for instance, Rossi and Sekhposyan (2014). Since, the visual inspection offers straightforward conclusions, I do not resort to these methods.

¹⁷Wolters (2015) demonstrates that this problem also applies to estimated DSGE models.

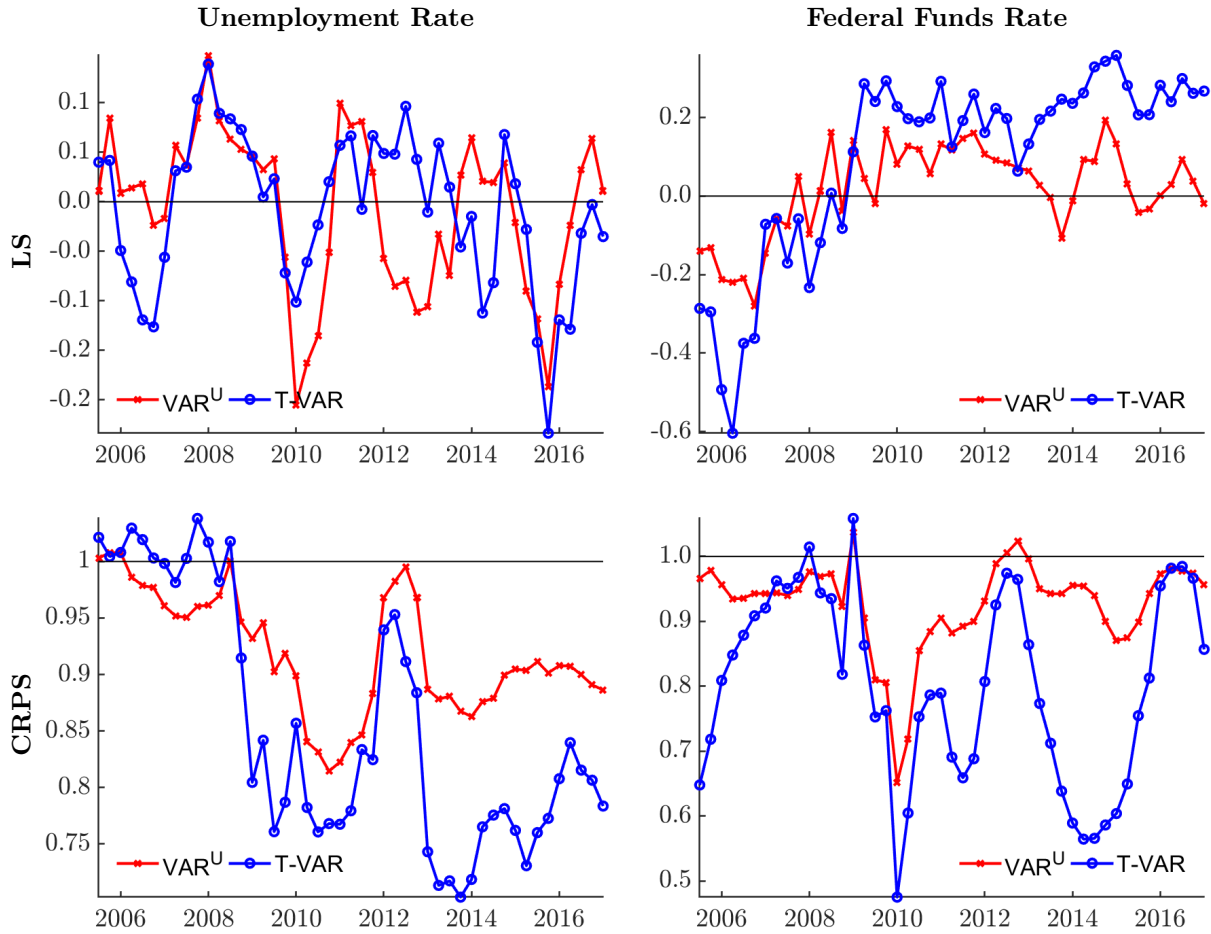
Table 3: CRPS and LS

Specification	CRPS				LS			
	$h = 1$	$h = 2$	$h = 3$	$h = 4$	$h = 1$	$h = 2$	$h = 3$	$h = 4$
Inflation								
VAR	0.50	1.91	3.62	5.53	-2.17	-3.20	-3.75	-4.12
VAR ^U	0.89	0.97	1.02	1.09●	0.04	0.10●	-0.04	-0.05
T-VAR	1.60●	3.20●	3.73●	4.24●	-0.36●	-1.23●	-1.29●	-1.31●
Output growth								
VAR	3.55	10.40	5.73	5.94	-3.61	-4.72	-4.28	-4.30
VAR ^U	1.00	0.99●	0.98●	0.99●	0.01	0.07●	0.01	-0.01
T-VAR	0.92●	1.59●	2.26●	3.03●	0.19●	-0.35●	-0.73●	-1.00●
Investment growth								
VAR	16.64	54.25	32.74	34.62	-5.38	-6.53	-6.11	-6.07
VAR ^U	0.97●	0.97●	0.98●	0.98●	-0.02	0.02	0.07	0.07
T-VAR	1.10●	1.79●	2.46●	3.12●	-0.04	-0.55●	-0.83●	-1.02●
Consumption growth								
VAR	3.26	7.77	12.38	15.79	-3.56	-4.43	-4.86	-5.10
VAR ^U	0.96●	0.95●	0.97●	0.96●	0.05●	0.04	0.03	0.01
T-VAR	0.87●	1.61●	2.14●	2.75●	0.23●	-0.41●	-0.67●	-0.96●
Unemployment rate								
VAR	0.15	0.47	0.76	1.10	-1.99	-2.29	-2.49	-2.67
VAR ^U	0.89●	0.92●	0.92●	0.91●	-0.01	0.05●	0.07●	0.07●
T-VAR	0.84●	1.00	0.94	0.89●	-0.00	-0.05	0.02	0.11●
Federal funds rate								
VAR	0.36	1.09	1.77	2.42	-2.14	-2.73	-3.12	-3.39
VAR ^U	0.91●	1.04	1.05	1.07	0.02	0.01	0.02	-0.03
T-VAR	0.79●	0.84●	0.93●	0.99	0.10●	0.16●	0.14●	0.13●

Notes: VAR and VAR^U denote the linear VAR without macro uncertainty and including macro uncertainty, respectively. T-VAR refers to the threshold VARs. The scores are reported in absolute terms for the benchmark model. For the remaining models LSs are expressed in differences to the benchmark and CRPSs in ratios to the benchmark model. A positive difference and a ratio below unity indicate the model outperforms the benchmark. ●, • and • denote significance on the 5%, 10% and 15% level, respectively, according to a t-test on the average difference in scores relative to the benchmark model with Newey-West standard errors. Sample: 1960Q3–2017Q4.

data. At higher horizons, however, the densities are again too wide. Regarding unemployment rate forecasts, the PITs of each model are closer to uniformity for $h = 1$ and $h = 2$; both the lower and the upper percentiles of the actual distribution are captured by the models. At the remaining horizons, the models again overestimate the actual uncertainty. The PITs for the interest rate forecasts appear to be right skewed, and thus missing the left tail of the actual distribution. The latter stems from the phase of extraordinary low interest rates at the end of the sample, which are barely captured by the models. Only the VAR^U is able to generate forecasts

Figure 5: Forecast Performance Over Time – Density Forecasts



Note: The figure displays log scores (upper panel) and continuous ranked probability scores (bottom panel) computed as a four-quarter moving average over the forecast sample for unemployment and federal funds rate forecasts.

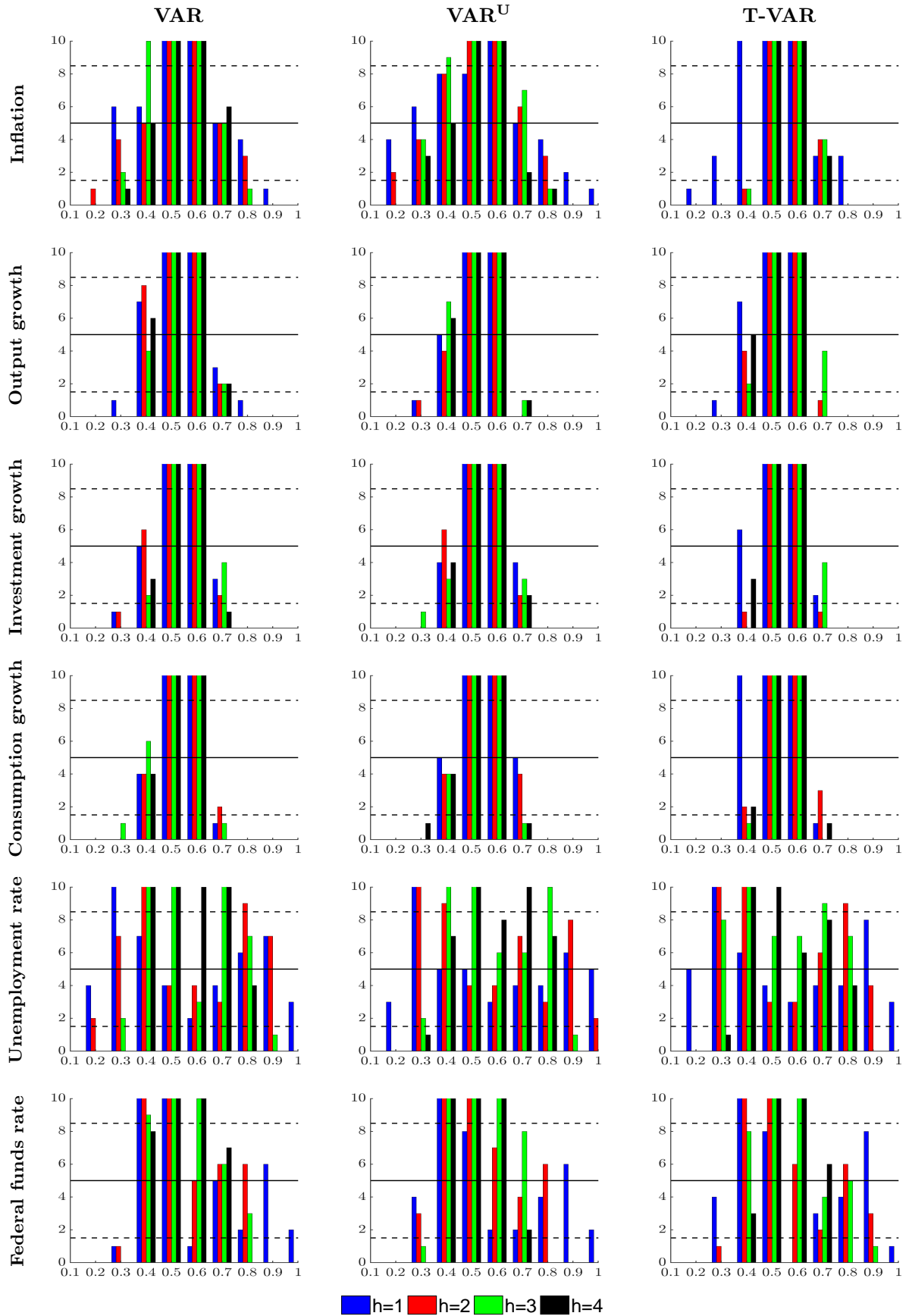
corresponding to the lower percentiles. Jointly with the results from Table 3, the evaluation of the PITs suggests that estimating regime-dependent covariance matrices with respect to the prevailing level of uncertainty helps calibrating accurate predictive densities.

6 Conclusion

Evidence from studies on the effects of uncertainty shocks suggests that uncertainty impacts real economy variables and that these impacts depend on the prevailing level of uncertainty . This paper answers the questions of whether these insights can be used to achieve more accurate forecasts from VAR models and whether one has to account for nonlinearities to achieve this goal. I compared the forecast performance of different Bayesian VAR specifications. The analysis provides four main results. First, in a linear setting, point forecast accuracy cannot be significantly improved by considering information from the macroeconomic uncertainty index. Second, accounting for regime-specific model dynamics depending on the level of uncertainty

improves the point forecast accuracy for unemployment rate and interest rate forecasts, while the accuracy for real activity variables deteriorates. Third, predictive densities benefit significantly from the macroeconomic uncertainty index both in a linear and nonlinear setting. However, the nonlinear model outperforms the linear models, especially at short horizons. The largest gains are obtained for unemployment rate forecasts. Moreover, and in contrast to the point forecasts, the threshold VAR also provides strong improvements for the predictive densities of the real activity variables. Finally, I document substantial variation in the models' predictive ability. In particular, during episodes of high uncertainty, the T-VAR provides strong gains in forecast accuracy with respect to the predictive densities. Thus, it can serve as a complement to existing approaches in arriving at a better picture of the actual uncertainty surrounding the point estimate in times of high uncertainty and especially for unemployment forecasts.

Figure 6: Probability Integral Transform (PITs)



Note: The figure displays the cdf of the probability integral transforms (PITs). Solid and dashed black lines denote uniformity and 90% confidence bands, respectively.

References

- ABEL, A. B. (1973). Optimal investment under uncertainty. *American Economic Review*, **73** (1), 228–233.
- ADOLFSON, M., LINDÉ, J. and VILLANI, M. (2007). Forecasting Performance of an Open Economy DSGE Model. *Econometrics Review*, **26** (2-4), 289–328.
- ALESSANDRI, P. and MUMTAZ, H. (2017). Financial conditions and density forecasts for US output and inflation. *Review of Economic Dynamics*, **24**, 66–78.
- and — (2018). Financial Regimes and Uncertainty Shocks. *Journal of Monetary Economics*, **forthcoming**.
- ARELLANO, C., BAI, Y. and KEHOE, P. (2012). *Financial Markets and Fluctuations in Uncertainty*. March, Federal Reserve Bank of Minneapolis Research Department Staff Report.
- AUERBACH, A. J. and GORODNICHENKO, Y. (2012). Measuring the Output Responses to Fiscal Policy. *American Economic Journal: Economic Policy*, **4** (2), 1–27.
- BACHMANN, R. and BAYER, C. (2013). Wait-and-see business cycles? *Journal of Monetary Economics*, **60** (6), 704–719.
- , ELSTNER, S. and SIMS, E. R. (2013). Uncertainty and economic activity: Evidence from business survey data. *American Economic Journal: Macroeconomics*, **5** (2), 217–249.
- BAKER, S. R., BLOOM, N. and DAVIS, S. J. (2016). Measuring Economic Policy Uncertainty. *The Quarterly Journal of Economics*, **131** (4), 1593–1636.
- BALCILAR, M., GUPTA, R. and SEGNON, M. (2016). The role of economic policy uncertainty in predicting US recessions: A mixed-frequency Markov-switching vector autoregressive approach. *Economics: The Open-Access, Open-Assessment E-Journal*, **10** (2016-27), 1–20.
- BAÑBURA, M., GIANNONE, D. and REICHLIN, L. (2010). Large Bayesian Vector Auto Regressions. *Journal of Applied Econometrics*, **25** (1), 71–92.
- BARNETT, A., MUMTAZ, H. and THEODORIDIS, K. (2014). Forecasting UK GDP growth and inflation under structural change. A comparison of models with time-varying parameters. *International Journal of Forecasting*, **30** (1), 129–143.
- BASU, S. and BUNDICK, B. (2017). Uncertainty Shocks in a Model of Effective Demand. *Econometrica*, **85** (3), 937–958.
- BEKIROU, S., GUPTA, R. and PACCAGNINI, A. (2015). Oil price forecastability and economic uncertainty. *Economics Letters*, **132**, 125–128.
- and PACCAGNINI, A. (2015). Estimating point and density forecasts for the US economy with a factor-augmented vector autoregressive DSGE model. *Studies in Nonlinear Dynamics & Econometrics*, **19** (2), 107–136.

- BERG, T. O. (2016). Multivariate Forecasting with BVARs and DSGE Models. *Journal of Forecasting*, **35**, 718–740.
- (2017a). Business Uncertainty and the Effectiveness of Fiscal Policy in Germany. *Macroeconomic Dynamics*, **forthcoming**.
- (2017b). Forecast Accuracy of a BVAR under Alternative Specifications of the Zero Lower Bound. *Studies in Nonlinear Dynamics & Econometrics*, **21** (2), 1–29.
- and HENZEL, S. R. (2015). Point and density forecasts for the euro area using Bayesian VARs. *International Journal of Forecasting*, **31** (4), 1067–1095.
- BERNANKE, B. S. (1983). Irreversibility, uncertainty, and cyclical investment. *The Quarterly Journal of Economics*, **98** (1), 85–106.
- BIJSTERBOSCH, M. and GUÉRIN, P. (2013). Characterizing very high uncertainty episodes. *Economics Letters*, **121** (2), 239–243.
- BLOOM, N. (2009). The impact of uncertainty shocks. *Econometrica*, **77** (3), 623–685.
- BONCIANI, D. and VAN ROYE, B. (2016). Uncertainty shocks, banking frictions and economic activity. *Journal of Economic Dynamics & Control*, **73**, 200–219.
- BORN, B. and PFEIFER, J. (2014). Policy risk and the business cycle. *Journal of Monetary Economics*, **68**, 68–85.
- and — (2017). *Uncertainty-driven Business Cycles: Assessing the Markup Channel*. CESifo Working Paper 6303, Center for Economic Studies and Ifo Institute (CESifo), Munich.
- CABALLERO, R. and PINDYCK, R. S. (1996). Uncertainty, investment, and industry evolution. *International Economic Review*, **37** (3), 641–662.
- CAGGIANO, G., CASTELNUOVO, E. and FIGUERES, J. M. (2017). Economic policy uncertainty and unemployment in the United States: A nonlinear approach. *Economics Letters*, **151**, 31–34.
- , — and GROSHENNY, N. (2014). Uncertainty shocks and unemployment dynamics in U.S. recessions. *Journal of Monetary Economics*, **67**, 78–92.
- CALDARA, D., FUENTES-ALBERO, C., GILCHRIST, S. and ZAKRAJŠEK, E. (2016). The macroeconomic impact of financial and uncertainty shocks. *European Economic Review*, **88** (C), 185–207.
- CARRIERO, A., CLARK, T. E. and MARCELLINO, M. (2013). Bayesian VARs: Specification Choices and Forecast Accuracy. *Journal of Applied Econometrics*, **30** (1), 46–73.
- , KAPETANIOS, G. and MARCELLINO, M. (2009). Forecasting exchange rates with a large Bayesian VAR. *International Journal of Forecasting*, **25** (2), 400–417.

- , MUMTAZ, H., THEODORIDIS, K. and THEOPHILOPOULOU, A. (2015). The Impact of Uncertainty Shocks under Measurement Error: A Proxy SVAR Approach. *Journal of Money, Credit and Banking*, **47** (6), 1223–1238.
- CASTELNUOVO, E. and PELLEGRINO, G. (2018). Uncertainty-dependent effects of monetary policy shocks: A new-Keynesian interpretation. *Journal of Economic Dynamics and Control*, **93**, 277 – 296.
- CHEN, C. W. S. and LEE, J. C. (1995). Bayesian inference of threshold autoregressive models. *Journal of Time Series Analysis*, **16** (5), 483–492.
- CHIU, C.-W. J., MUMTAZ, H. and PINTÉR, G. (2017). Forecasting with VAR models: Fat tails and stochastic volatility. *International Journal of Forecasting*, **33** (4), 1124–1143.
- CHRISTIANO, L., MOTTO, R. and ROSTAGNO, M. (2014). Risk shocks. *American Economic Review*, **104** (1), 27–65.
- CLARK, T. E. (2012). Real-Time Density Forecasts From Bayesian Vector Autoregressions With Stochastic Volatility. *Journal of Business & Economic Statistics*, **29** (3), 327–341.
- and RAVAZZOLO, F. (2015). Macroeconomic forecasting performance under alternative specifications of time-varying volatility. *Journal of Applied Econometrics*, **30** (4), 551–575.
- COGLEY, T. and SARGENT, T. J. (2001). Evolving Post-World War II US inflation Dynamics. In *NBER Macroeconomics Annual 2001, NBER Chapters*, vol. 16, National Bureau of Economic Research, Inc, pp. 331–373.
- D’AGOSTINO, A., GAMBETTI, L. and GIANNONE, D. (2013). Macroeconomic forecasting and structural change. *Journal of Applied Econometrics*, **28** (1), 82–101.
- DIEBOLD, F. X., GUNTHER, T. A. and TAY, A. S. (1998). Evaluating density forecasts with applications to financial risk management. *International Economic Review*, **39** (4), 863–883.
- and MARIANO, R. S. (1995). Comparing Predictive Accuracy. *Journal of Business & Economic Statistics*, **13** (3), 253–263.
- DOAN, T., LITTERMAN, R. and SIMS, C. (1984). Forecasting and conditional projection using realistic prior distributions. *Econometric Reviews*, **3** (1), 1–100.
- FERNÁNDEZ-VILLAYERDE, J., GUERRÓN-QUINTANA, P., KUESTER, K. and RUBIO-RAMÍREZ, J. (2015). Fiscal volatility shocks and economic activity. *American Economic Review*, **105** (11), 3352–3384.
- FERRARA, L. and GUÉRIN, P. (2018). What are the macroeconomic effects of high-frequency uncertainty shocks? *Journal of Applied Econometrics*, **33** (5), 662–679.
- FOERSTER, A. T. (2014). The asymmetric effects of uncertainty. *Economic Review-Federal Reserve Bank of Kansas City*, **Q III**, 5–26.

- GERARD, H. and NIMARK, K. (2008). *Combining multivariate density forecasts using predictive criteria*. Economics Working Papers 1117, Department of Economics and Business, Universitat Pompeu Fabra.
- GEWEKE, J. and AMISANO, G. (2010). Comparing and evaluating Bayesian predictive distributions of asset returns. *International Journal of Forecasting*, **26** (2), 216–230.
- GIANNONE, D., LENZA, M. and PRIMICERI, G. E. (2015). Prior selection for vector autoregressions. *Review of Economics and Statistics*, **97** (2), 436–451.
- GILCHRIST, S., SIM, J. W. and ZAKRAJŠEK, E. (2014). *Uncertainty, financial frictions, and investment dynamics*. NBER Working Paper 20038, National Bureau of Economic Research, Inc.
- GNEITING, T. and RAFTERY, A. E. (2007). Strictly proper scoring rules, prediction, and estimation. *Journal of the American Statistical Association*, **102** (477), 359–378.
- and RANJAN, R. (2011). Comparing density forecasts using threshold and quantile weighted scoring rules. *Journal of Business & Economic Statistics*, **29** (3), 411–422.
- GOOD, I. J. (1952). Rational decisions. *Journal of the Royal Statistical Society. Series B (Methodological)*, **14** (1), 107–114.
- GROEN, J. J. J., PAAP, R. and RAVAZZOLO, F. (2013). Real-Time Inflation Forecasting in a Changing World. *Journal of Business & Economic Statistics*, **31** (1), 29–44.
- HARTMAN, R. (1972). The effects of price and cost uncertainty on investment. *Journal of Economic Theory*, **5** (2), 258–266.
- HARVEY, D., LEYBOURNE, S. and NEWBOLD, P. (1997). Testing the equality of prediction mean squared errors. *International Journal of Forecasting*, **13** (2), 281–291.
- HENZEL, S. R. and RENGEL, M. (2017). Dimensions of Macroeconomic Uncertainty: A Common Factor Analysis. *Economic Inquiry*, **55** (2), 843–877.
- HUBER, F. (2016). Density forecasting using Bayesian global vector autoregressions with stochastic volatility. *International Journal of Forecasting*, **32** (3), 818–837.
- JONES, P. M. and ENDERS, W. (2016). The Asymmetric Effects of Uncertainty on Macroeconomic Activity. *Macroeconomic Dynamics*, **20** (5), 1219–1246.
- JORE, A. S., MITCHELL, J. and VAHEY, S. P. (2010). Combining forecast densities from VARs with uncertain instabilities. *Journal of Applied Econometrics*, **25** (4), 621–634.
- JURADO, K., LUDVIGSON, S. C. and NG, S. (2015). Measuring uncertainty. *The American Economic Review*, **105** (3), 1177–1216.
- KADIYALA, K. R. and KARLSSON, S. (1997). Numerical Methods for Estimation and Inference in Bayesian VAR-Models. *Journal of Applied Econometrics*, **12** (2), 99–132.

- KILIAN, L. and VIGFUSSON, R. J. (2011). Are the responses of the U.S. economy asymmetric in energy price increases and decreases? *Quantitative Economics*, **2** (3), 419–453.
- KOOP, G. M. (2013). Forecasting with medium and large Bayesian VARs. *Journal of Applied Econometrics*, **28** (2), 177–203.
- , PESARAN, M. H. and POTTER, S. M. (1996). Impulse response analysis in nonlinear multivariate models. *Journal of Econometrics*, **74** (1), 119–147.
- LEDUC, S. and LIU, Z. (2016). Uncertainty shocks are aggregate demand shocks. *Journal of Monetary Economics*, **82**, 20–35.
- LITTERMAN, R. B. (1986). Forecasting with Bayesian vector autoregressions – five years of experience. *Journal of Business & Economic Statistics*, **4** (1), 25–38.
- MATHESON, J. E. and WINKLER, R. L. (1976). Scoring rules for continuous probability distributions. *Management Science*, **22** (10), 1087–1096.
- MCCRACKEN, M. W. and NG, S. (2016). Fred-md: A monthly database for macroeconomic research. *Journal of Business & Economic Statistics*, **34** (4), 574–589.
- MUMTAZ, H. and THEODORIDIS, K. (2015). The international transmission of volatility shocks: An empirical analysis. *Journal of the European Economic Association*, **13** (3), 512–533.
- and — (2018). The Changing Transmission of Uncertainty Shocks in the U.S. *Journal of Business & Economic Statistics*, **36** (2), 239–252.
- OI, W. Y. (1961). The desirability of price instability under perfect competition. *Econometrica*, **29** (1), 58–64.
- PANAGIOTELIS, A. and SMITH, M. (2008). Bayesian density forecasting of intraday electricity prices using multivariate skew t distributions. *International Journal of Forecasting*, **24** (4), 710–727.
- PIERDZIOCH, C. and GUPTA, R. (2017). *Uncertainty and Forecasts of U.S. Recessions*. Working Papers 201732, University of Pretoria, Department of Economics.
- POPESCU, A. and SMETS, F. R. (2010). Uncertainty, risk-taking, and the business cycle in germany. *Cesifo Economic Studies*, **56** (4/2010), 596–626.
- ROSENBLATT, M. (1952). Remarks on a multivariate transformation. *The Annals of Mathematical Statistics*, **23** (3), 470–472.
- ROSSI, B. and SEKHPOSYAN, T. (2014). Evaluating predictive densities of US output growth and inflation in a large macroeconomic data set. *International Journal of Forecasting*, **30** (3), 662–682.
- and — (2015). Macroeconomic uncertainty indices based on nowcast and forecast error distributions. *The American Economic Review*, **105** (5), 650–655.

- SEGNON, M., GUPTA, R., BEKIROU, S. and WOHAR, M. E. (2018). Forecasting US GNP growth: The role of uncertainty. *Journal of Forecasting*, **37** (5), 541–559.
- SIMS, C. A. (1993). A Nine-Variable Probabilistic Macroeconomic Forecasting Model. In J. H. Stock and M. W. Watson (eds.), *NBER Studies in Business: Business Cycles, Indicators, and Forecasting*, NBER Chapters, National Bureau of Economic Research, Inc, pp. 179–212.
- SMITH, M. S. and VAHEY, S. P. (2015). Asymmetric Forecast Densities for U.S. Macroeconomic Variables from a Gaussian Copula Model of Cross-Sectional and Serial Dependence. *Journal of Business & Economic Statistics*, **34** (3), 416–434.
- WOLTERS, M. H. (2015). Evaluating Point and Density Forecasts of DSGE Models. *Journal of Applied Econometrics*, **30** (1), 74–96.

Appendix

A Prior Implementation

For the prior implementation, I express the VAR(p) in (1) in companion form:

$$Y = XB + U, \quad (16)$$

with $Y = (y_1, \dots, y_T)'$, $X = (X_1, \dots, X_T)'$ with $X_t = (y'_{t-1}, \dots, y'_{t-p}, 1)'$, $U = (\varepsilon_1, \dots, \varepsilon_T)'$ and $B = (A_1, \dots, A_p, c)'$.

The normal-inverse Wishart prior takes the following form:

$$\Sigma \sim iW(\Psi, \underline{\alpha}) \quad \text{and} \quad \text{vec}(B)|\Sigma \sim N(\text{vec}(\underline{B}), \Sigma \otimes \underline{\Omega}), \quad (17)$$

where \underline{B} , $\underline{\Omega}$, $\underline{\alpha}$, and Ψ are functions of hyperparameters. To implement these prior beliefs, I follow Bańbura *et al.* (2010) and augment the dataset with dummy observations:

$$Y^{D,1} = \begin{pmatrix} \text{diag}(\delta_1 \sigma_1, \dots, \delta_n \sigma_n) / \lambda_1 \\ 0_{n(p-1) \times n} \\ \text{diag}(\sigma_1, \dots, \sigma_n) \\ 0_{1 \times n} \end{pmatrix} X^{D,1} = \begin{pmatrix} J_p \text{diag}(\sigma_1, \dots, \sigma_n) / \lambda_1 & 0_{np \times 1} \\ 0_{n \times np} & 0_{n \times 1} \\ 0_{1 \times np} & \epsilon \end{pmatrix}. \quad (18)$$

δ_1 to δ_n denote the prior means of the coefficients on the first lag. δ_i is set to one, implying a random walk prior for non-stationary variables, and set to zero for stationary variables. σ_1 to σ_n are scaling factors, which are set to the standard deviations from univariate autoregressions of the endogenous variables using the same lag length as in the VAR. I impose a flat prior on the intercept terms by setting ϵ to 1/10000. The hyperparameter λ_1 controls the overall tightness of the prior. Hence, with increasing λ_1 the degree of shrinkage declines.

The ‘‘sum-of-coefficients’’ prior imposes the restriction that the sum of the coefficients of the lags of the dependent variables sum up to unity, whereas the lags of other variables sum up to zero. It is implemented by the following dummy observations:

$$Y^{D,2} = \text{diag}(\delta_1 y_1, \dots, \delta_n y_n) / \lambda_2 \quad X^{D,2} = ((1_{1 \times p}) \text{diag}(\delta_1 \mu_1, \dots, \delta_n \mu_n) / \lambda_2 \quad 0_{n \times 1}), \quad (19)$$

where μ_i denotes the sample average of variable i . The degree of shrinkage is determined by the hyperparameter λ_2 . The prior becomes less informative for higher values of λ_2 .

The ‘‘co-persistence’’ prior allows for possibility of stable cointegration relations among the variables. Sims (1993) proposes to add the following dummy observations to the sample to implement the prior:

$$Y^{D,3} = \text{diag}(\delta_1 \mu_1, \dots, \delta_n \mu_2) \lambda_3 \quad X^{D,3} = ((1_{1 \times p}) \text{diag}(\delta_1 \mu_1, \dots, \delta_n \mu_2)) \lambda_3, \quad (20)$$

where λ_3 controls the degree of shrinkage of this prior. If λ_3 approaches zero, the prior becomes more tight. Defining $Y^* = [Y, Y^{D,1}, Y^{D,2}, Y^{D,3}]$, $X^* = [X, X^{D,1}, X^{D,2}, X^{D,3}]$, and

$U^* = [U, U^{D,1}, U^{D,2}, U^{D,3}]$ yields the augmented dataset, which is used for inference via:

$$Y^* = X^*B + U^*. \quad (21)$$

The posterior expectations are determined by an OLS regression of Y^* on X^* . The posterior takes the form:

$$\Sigma|\lambda, y \sim IW(\tilde{\Sigma}, T + n + 2) \quad \text{vec}(B)|\Sigma, \lambda, y \sim N(\text{vec}(\hat{B}), \Sigma \otimes (X^{*'}X^*)^{-1}), \quad (22)$$

where \hat{B} is the matrix of coefficients from the regression of Y^* on X^* , and $\tilde{\Sigma}$ is the corresponding covariance matrix. In sampling B , I follow Cogley and Sargent (2001) and discard draws leading to an unstable VAR.

B Determining the Degree of Shrinkage

The forecast performance of Bayesian VARs tends to be sensitive with respect to the choice of the hyperparameters, which in turn have to be chosen with care. The vector Λ collecting the hyperparameters consists of three elements: the overall tightness of the prior (λ_1), the extent to which the sum of coefficients on the lags of a variable are forced to unity (λ_2), and the extent to which co-persistence restrictions are imposed on the VAR coefficients (λ_3). Following the specifications (18), (19) and (20), the smaller λ_i , the more informative the prior. To get a reasonable degree of shrinkage, I apply the hierarchical, fully Bayesian procedure of Giannone *et al.* (2015).¹⁸ The posterior for such a hierarchical prior is obtained by applying Bayes' law

$$p(\Lambda|y) \propto p(y|\Lambda)p(\Lambda) \quad (23)$$

where $p(\lambda)$ is the prior density of the hyperparameters – the so-called hyperprior. The marginal likelihood of the model $p(y|\Lambda)$ is given by:

$$p(y|\lambda) = \int p(y|\theta, \Lambda)p(\theta|\Lambda)d\theta \quad (24)$$

with θ denoting the vector of model parameters. As shown by Carriero *et al.* (2013) and Giannone *et al.* (2015), using conjugate priors results in a closed-form solution for the marginal likelihood:

$$p(Y|\Lambda) = k^{-1} \times |\Psi + (Y - X\underline{B})'(I + X\underline{\Omega}X')^{-1}(Y - X\underline{B})|^{-\frac{\alpha+T}{2}} \quad (25)$$

$$\text{with: } k = \pi^{\frac{Tn}{2}} \times |(I + X\underline{\Omega}X')^{-\frac{n}{2}} \times |\Psi|^{-\frac{\alpha}{2}} \times \frac{\Gamma(\frac{\alpha}{2})}{\Gamma(\frac{T+\alpha}{2})} \quad (26)$$

¹⁸Apart from this procedure, one can also determine the degree of shrinkage based on the in-sample fit compared to a parsimonious VAR (Bańbura *et al.*, 2010), or by maximizing the marginal likelihood at each point in time (Carriero, Clark and Marcellino, 2013). A comparison of these methods with respect to forecast accuracy is provided by Berg and Henzel (2015).

where $\underline{B} = (X^{D'} X^D)^{-1} X^{D'} Y^D$, $\underline{\Omega} = (X^{D'} X^D)^{-1}$, and $\underline{\Psi} = (Y^D - X^D \underline{B})^{-1} (Y^D - X^D \underline{B})$. $\Gamma(\cdot)$ denotes the n -variate gamma distribution and $\underline{\alpha} = n + 2$ in order to ensure existence of the prior mean of Σ (Kadiyala and Karlsson, 1997). The hyperpriors for $\lambda_1, \lambda_2, \lambda_3$, i.e., the priors for the hyperparameters, reflect the knowledge about the values of λ_i . I follow Giannone *et al.* (2015) by choosing uninformative priors using Gamma densities with modes equal to 0.2, 1, and 1 and standard deviations equal to 0.4, 1, and 1, respectively. I employ a Metropolis-Hastings step to simulate the distribution. Define D and R as the number of discarded and retained draws, respectively. The algorithm works as follows:

1. At iteration $k = 1$ initialize Λ at the posterior mode, which can be obtained by numerical optimization.¹⁹
2. Draw a candidate value Λ^* for the hyperparameters from a random walk proposal distribution $\Lambda^* \sim N(\delta^{k-1}, cH^{-1})$, where c is a scaling factor calibrated to ensure an acceptance rate of roughly 20% and H^{-1} is the inverse of the Hessian evaluated at the posterior mode.
3. Set $\Lambda^k = \Lambda^*$ with probability

$$\alpha^k = \min \left\{ 1, \frac{p(\Lambda^*|y)}{p(\Lambda^{k-1}|y)} \right\}. \quad (27)$$

If $k < D$ redo, otherwise continue.

4. Conditional on Λ^k draw Σ^k and β^k from their posteriors given by (22).
5. Generate $\varepsilon_{T+1}^k, \dots, \varepsilon_{T+h}^k$ from $\varepsilon_t \sim N(0, \Sigma^k)$ and calculate h -step-ahead forecasts recursively

$$\hat{y}_{T+h}^k = c^k + \sum_{i=1}^{h-1} A_i^k \hat{y}_{T+h-i}^k + \sum_{i=h}^p A_i^k \hat{y}_{T+h-i}^k + u_{T+h}^k. \quad (28)$$

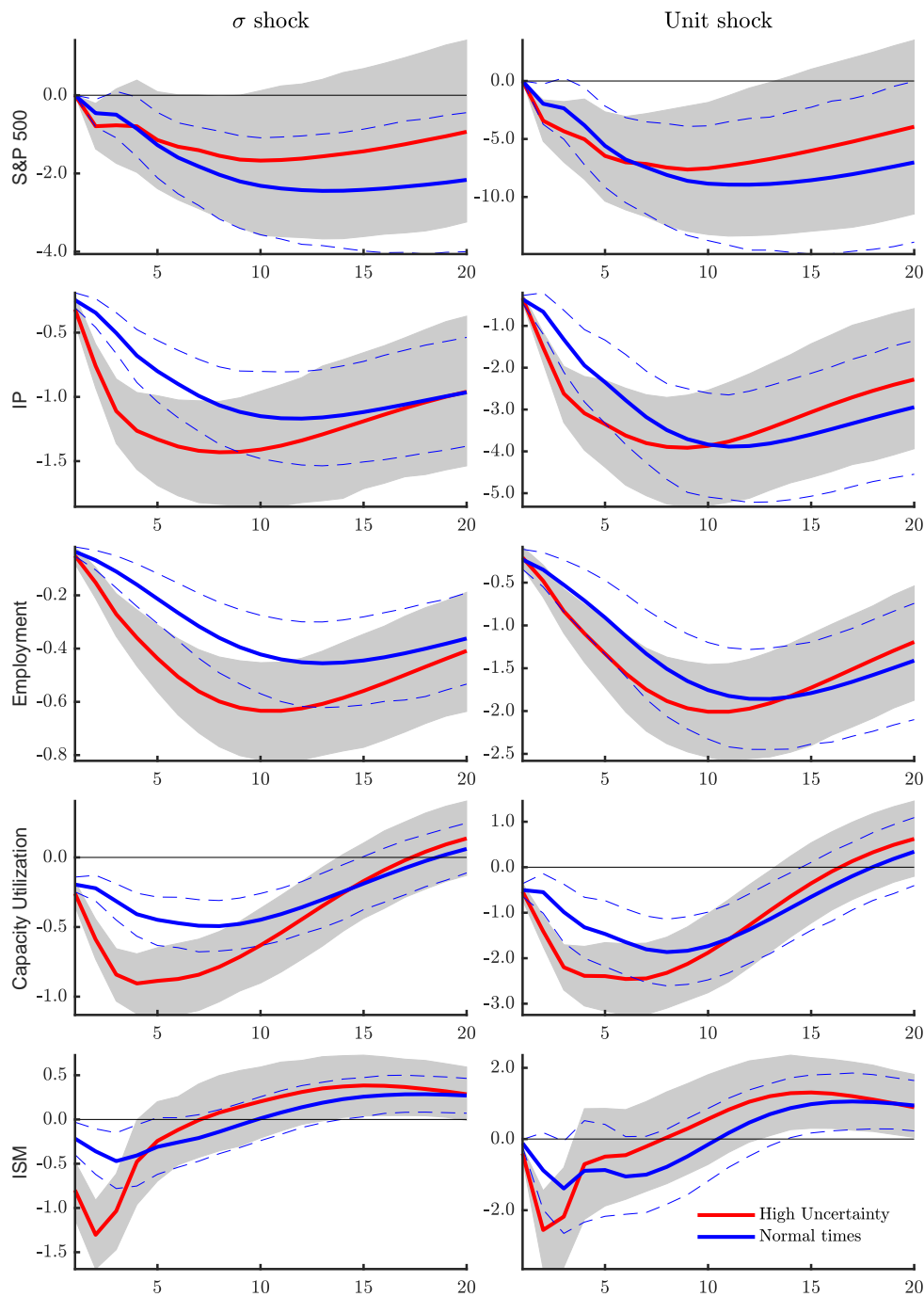
6. Iterate these steps until $j = D + R$.

Note that since Λ is independent of Σ and β , one can draw Λ until the sampler converges and subsequently draw successively Σ and β . Applying this algorithm yields R h -step-ahead forecasts from the joint posterior distribution. From 25000 draws, 5000 are used for inference.

¹⁹I use the Matlab `globalsearch` class based on the routine `fmincon` to obtain a global maximum.

C Generalized Impulse Responses

Figure 7: Regime-Dependent Impact to an Uncertainty Shock



Note: The figure displays the impact of an uncertainty shock to selected variables in normal times and in times of high uncertainty. The left column refers to a one standard deviation innovation while the right column depicts a unit shock. The responses are generated using a recursive identification scheme with uncertainty ordered second. Gray shaded areas and dashed blue lines refer to 68% error bands. The macro uncertainty index enters the model standardized.

ifo Working Papers

- No. 264 Wohlrabe, K., F. de Moya Anegon and L. Bornmann, How efficiently produce elite US universities highly cited papers? A case study based on input and output data, October 2018.
- No. 263 Schwefer, M., Sitting on a Volcano: Domestic Violence in Indonesia Following Two Volcano Eruptions, September 2018.
- No. 262 Vandreï, L., Does Regulation Discourage Investors? Sales Price Effects of Rent Controls in Germany, June 2018.
- No. 261 Sandkamp, A.-N., The Trade Effects of Antidumping Duties: Evidence from the 2004 EU Enlargement, June 2018.
- No. 260 Corrado, L. and T. Schuler, Financial Bubbles in Interbank Lending, April 2018.
- No. 259 Löffler, M., A. Peichl and S. Siegloch The Sensitivity of Structural Labor Supply Estimations to Modeling Assumptions, March 2018.
- No. 258 Fritzsche, C. and L. Vandreï, Causes of Vacancies in the Housing Market – A Literature Review, March 2018.
- No. 257 Potrafke, N. and F. Rösel, Opening Hours of Polling Stations and Voter Turnout: Evidence from a Natural Experiment, February 2018.
- No. 256 Hener, T. and T. Wilson, Marital Age Gaps and Educational Homogamy – Evidence from a Compulsory Schooling Reform in the UK, February 2018.
- No. 255 Hayo, B. and F. Neumeier, Households' Inflation Perceptions and Expectations: Survey Evidence from New Zealand, February 2018.
- No. 254 Kauder, B., N. Potrafke and H. Ursprung, Behavioral determinants of proclaimed support for environment protection policies, February 2018.

- No. 253 Wohlrabe, K., L. Bornmann, S. Gralka und F. de Moya Anegon, Wie effizient forschen Universitäten in Deutschland, deren Zukunftskonzepte im Rahmen der Exzellenzinitiative ausgezeichnet wurden? Ein empirischer Vergleich von Input- und Output-Daten, Februar 2018.
- No. 252 Brunori, P., P. Hufe and D.G. Mahler, The Roots of Inequality: Estimating Inequality of Opportunity from Regression Trees, January 2018.
- No. 251 Barrios, S., M. Dolls, A. Maftai, A. Peichl, S. Riscado, J. Varga and C. Wittneben, Dynamic scoring of tax reforms in the European Union, January 2018.
- No. 250 Felbermayr, G., J. Gröschl and I. Heiland, Undoing Europe in a New Quantitative Trade Model, January 2018.
- No. 249 Fritzsche, C., Analyzing the Efficiency of County Road Provision – Evidence from Eastern German Counties, January 2018.
- No. 248 Fuest, C. and S. Sultan, How will Brexit affect Tax Competition and Tax Harmonization? The Role of Discriminatory Taxation, January 2018.
- No. 247 Dorn, F., C. Fuest and N. Potrafke, Globalization and Income Inequality Revisited, January 2018.
- No. 246 Dorn, F. and C. Schinke, Top Income Shares in OECD Countries: The Role of Government Ideology and Globalization, January 2018.
- No. 245 Burmann, M., M. Drometer and R. Méango, The Political Economy of European Asylum Policies, December 2017.
- No. 244 Edo, A., Y. Giesing, J. Öztunc and P. Poutvaara, Immigration and Electoral Support for the Far Left and the Far Right, December 2017.
- No. 243 Enzi, B., The Effect of Pre-Service Cognitive and Pedagogical Teacher Skills on Student Achievement Gains: Evidence from German Entry Screening Exams, December 2017.